RESEARCH ARTICLE

The feasibility of cost-effective manufacturing activated carbon derived from walnut shells for large-scale CO_2 capture

Zahra Asadi-Sangachini[1] · Mohsen Mohammadi Galangash[1] · Habibollah Younesi[2] · Mohsen Nowrouzi[3]

Abstract

The economic potential of activated carbon (AC) synthesis from walnut shell biomass for CO_2 capture was evaluated in the present study. For this purpose, the chemical activation was employed to manufacture ACs and the effect of different impregnation ratios of activation agents, comprising KOH (KH) and H_3PO_4 (HP), onto the properties of fabricated ACs was examined. The obtained results demonstrated that the synthesized AC by HP activation with an impregnation ratio of 1:2.5, which was identified as HP2.5, possesses the highest surface area (1512.6 m^2/g), micropore volume percentage (74.65%), and CO_2 adsorption (3.55 mmol/g) at 1 bar and 30 °C. Moreover, the equilibrium CO_2 adsorption data for HP2.5 were better fitted with the Freundlich model, indicating the multilayer CO_2 adsorption onto the heterogeneous AC surface dominantly through a physisorption process. In addition, the economic estimations revealed a cost of about \$1.83/kg for the ultimate production that was significantly lower than the most of available CACs in the market. Therefore, walnut shells can be considered as a cost-effective and promising biomass source from a scale-up point of view.

Keywords CO_2 adsorption · Activated carbon · Walnut shells · Cost estimation

Introduction

The intensification of the global warming phenomenon due to the effect of greenhouse gas emissions from man-made resources is known as one of the greatest challenges of the environment in the present era. Among all effective gases in the creation and intensification of the global warming phenomenon, CO_2 emissions have demonstrated a more significant role in its escalation because of its more widespread sources (Ello et al. 2013). Therefore, extensive efforts are being performed to explore the best eco-environmentally friendly approach to prevent or reduce these emissions (Pal and Deb 2014). The broad range of technologies and procedures is proposed to attain this goal, and there is the strongest consensus on the solid adsorbents among those. Therefore, the use of typical solid absorbents includes activated carbon (AC), graphene, silica gel, exchangeable ion resins, zeolites, mesoporous silica, and metal oxides, and modified surface porous materials are recommended in the post-combustion capture of CO_2 (Nowrouzi et al. 2018). In a large-scale application, AC has been brought to close attention thanks to the engineering potential of its characteristics and the infinite availability of its sources to synthesis it according to the eco-environmental criteria. AC is a microcrystalline and non-graphite carbon form with a considerable porosity and a high specific surface area. The adsorption potential of different forms of ACs is extremely depended on its fundamental characteristics, e.g., surface area, porosity volume, and surface functional groups (Goel et al. 2016). However, the price of the final product is one of the most key parameters to welcome the industries' owners. Therefore, considering this fundamental attitude, the different lignocellulosic precursors are being investigated to

✉ Mohsen Mohammadi Galangash
m_mohammadi@guilan.ac.ir

✉ Habibollah Younesi
hunesi@modares.ac.ir; hunesi@yahoo.com

✉ Mohsen Nowrouzi
mohsennorouzi@pgu.ac.ir; mohsennorouzi@yahoo.com

[1] Department of Environmental Science, Faculty of Natural Resources, University of Guilan, Rasht, Guilan, Iran

[2] Department of Environmental Science, Faculty of Natural Resources, Tarbiat Modares University, P.O. Box 46414-356, Noor, Iran

[3] Department of Marine Environment, Faculty of Marine Science and Technology, Persian Gulf University, Bushehr 75169-13798, Iran

achieve a precursor with the highest economic benefits and the least environmental impact (Nowrouzi et al. 2017b). With this attitude, the goal of the present study is to focus a schematically plan view for large-scale and cost-effective production of AC on applying various environmental treatments and remediation, especially in CO_2 capture.

Walnut shells are chosen to manufacture AC and adsorb CO_2 in the present study due to its unique approved properties such as high density, high cellulose content, ease of access, and cost-effectiveness (Yang and Qiu 2010). However, AC is synthesized by two different approaches: physical activation and chemical activation. Today, chemical activation is preferable in most studies because of some advantages comprising lower applied temperature, shorter running time, higher carbon yield, and no formation of tar and volatile matter. In addition, different activating agents can be utilized to chemical activation which among those are KH and HP that are most widely used since they resulted in high surface areas and high yields (Heidari et al. 2014b). To the best of authors' knowledge, the cost estimation of synthesis AC derived from walnut shells, as an accessible and cost-effective precursor, with the aim of the large-scale CO_2 capture is not well documented. Therefore, the main objective of the present research was to figure out a facile, an economical and practical approach to manufacture an attractive adsorbent for polluting industry owners and highlight their possible application for CO_2 adsorption purposes. To attain this purpose, the physical properties of walnut shell biomass were characterized, the optimization process was performed using different ratios of activating agents, e.g., HP and KH, and eventually, the influence of different temperatures onto a CO_2 adsorption capacity by the optimized ACs were evaluated.

Materials and methods

Materials

Iranian walnut shells were collected from the trees of Tuyserkan city in Hamadan province. This material was first crushed and then dried at 70 °C, ground, and sieved to attain a particle size in the range of 0.4–0.8 mm. Afterward, its characteristics containing ash content, volatile matter, fixed carbon, and moisture content were specified by ASTM standard test methods (D3176). The elemental analysis (C, H, N, S, and O) was performed by a Carlo Erba elemental analyzer (Flash EA 1112, USA). Additionally, the chemicals for preparation of AC such as phosphoric acid (H_3PO_4) and potassium hydroxide (KOH) applied in this research were purchased from the Merck Company (Germany).

Pyrolysis experiment

The procedure of AC synthesis and CO_2 adsorption process by the volumetric method is shown in Fig. 1. In the first step of AC preparation, the precursor was carbonized to produce char at the temperature 600 °C, based on the thermogravimetric analysis (TGA) results. Then, a known weight of the char was mixed with different impregnation ratios of HP and KH as activating agents (0.75, 1, 1.5, 2, 2.5:1 activating agent:precursor w/w). The pyrolysis process was performed in a stationary horizontal stainless steel tube furnace adopting the procedure described below: a weighed amount of impregnated sample was placed in the reactor and was heated at a heating rate of 10 °C/min under an N_2 atmosphere (99.999%) at the flow rate of 140 standard mL/min (STP) with holding time of 2.5 h, at a temperature of 550 °C for acidic samples and 900 °C for alkali samples. The selection of activation temperature in each case was conducted according to the nature of the activating agent and literature reviews (Ello et al. 2013; Heidari et al. 2014a). After activation, the samples were cooled down to the room temperature under an N_2 atmosphere and then removed from the reactor. Subsequently, the samples were washed successively with hot and cold distilled water until the wash water reached a pH of 6–7. Ultimately, these samples were dried for 24 h at 110 °C prior to analysis (Heidari et al. 2014b).

Characterization of the ACs

The textural characterization of AC samples was carried out by conducting N_2 adsorption/desorption at −196 °C using a Micrometrics ASAP2020 analyzer (USA). Before adsorption measurements, all samples were degassed at 523 K under vacuum for at least 12 h. The Brunauer-Emmett-Teller (BET)-specific areas were determined using the BET method from adsorption data in the relative pressure (P/P_0) range of 0.001–0.3. Total pore volume was measured by the amount of nitrogen adsorbed at P/P_0 0.99. MP (micropore analysis) method was applied to measure the micropore volume, while the mesopore volume was calculated by subtracting micropore volumes from the total pore volume. The mesopore distribution was estimated using the Barrett-Joyner-Halenda (BJH) method. The surface functional groups of the AC samples were determined by attenuated total reflection Fourier transform infrared (ATR-FTIR) spectroscopy (FTIR – AVATAR 370, Thermo Nicolet, USA). The spectra were recorded between 4000 and 400 cm^{-1}, and the potassium bromide (KBr) pellet (*Merck*, Darmstadt, Germany) was used as the reference specimen. The surface morphology of the ACs was observed using scanning electron microscopy (SEM, Model S-4800, Hitachi Co., Japan). The AC samples were enclosed with gold by a gold sputtering device to allow for better visibility of the surface morphology. TGA of the Persian ironwood biomass
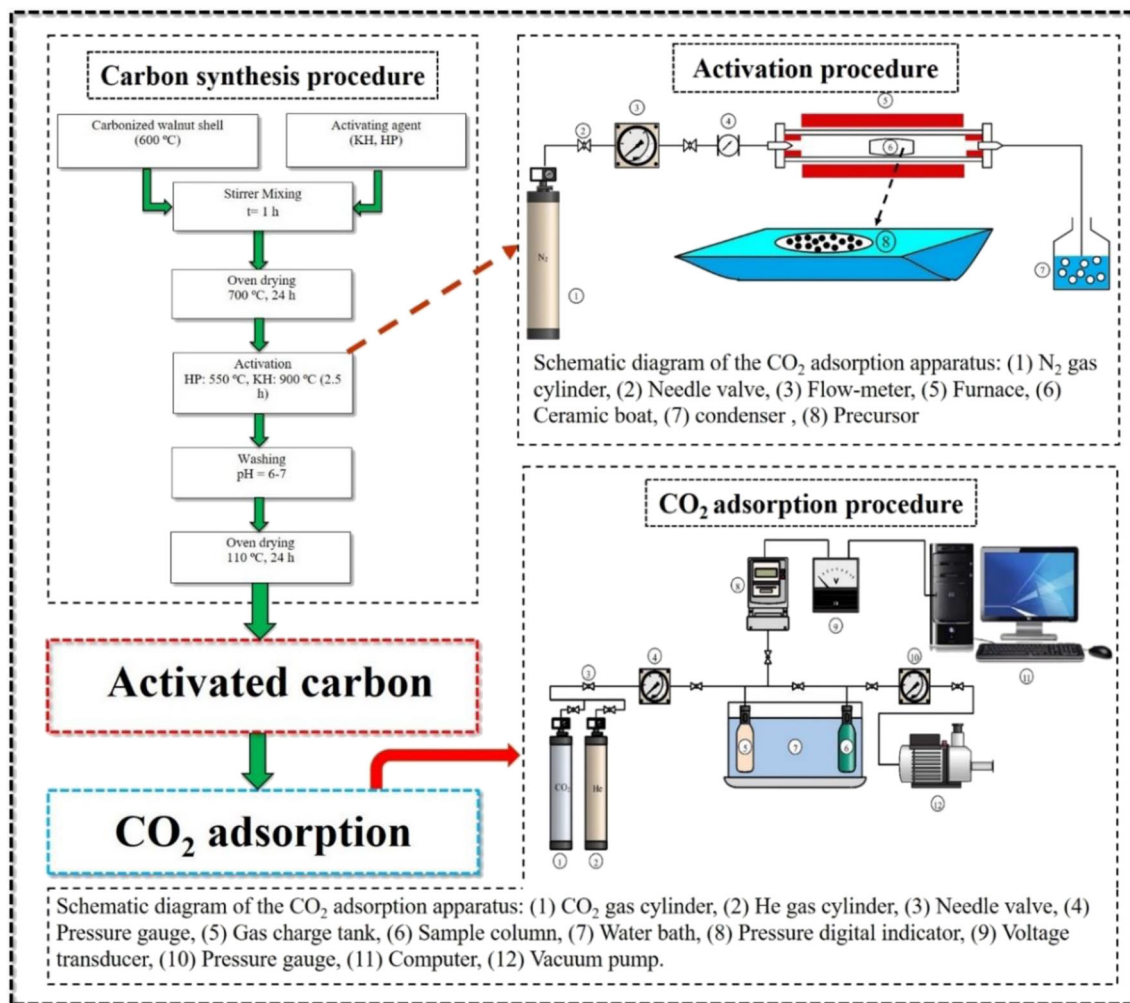
Fig. 1 Schematic diagram of AC synthesis and CO_2 adsorption

was carried out by using a thermogravimetric analyzer (STA 1500, Rheometric Scientific) under the N_2 atmosphere, from room temperature to 800 °C at the heating rate of 10 °C/min. The chemical composition of ACs was determined using CHNSO Elemental Analyzer (Flash EA 1112, USA). The elemental analysis only estimated the carbon, hydrogen, nitrogen, and sulfur content of the samples while the oxygen content was obtained from subtracting the sum of the above elements from 100.

CO_2 adsorption measurement

High purity CO_2 and He gases (99.999%) were purchased from a national gas company (Iran) and utilized for adsorption isotherm measurement. The CO_2 adsorption experiments on the ACs were performed by using volumetric adsorption set-up. The clear schematic diagram of applied apparatus in the present study is previously published by Nowrouzi et al. (2017b, 2018). However, it included two stainless steel sample cells (an adsorption cell and a gas cell), a set of valves, and

a couple of high-precision pressure transducers (maximum pressure 60 bars). The gas and adsorption cell volumes were 144 mL and 30 mL, respectively. In order to keep the temperature constant during the gas adsorption experiment, the gas cell and the adsorption cell were placed in a thermostatic water bath along with a water circulating system (77960 Seelbach, Julabo Co, Germany). Furthermore, before starting each CO_2 adsorption experiment, the setup was leak tested using helium gas (He) at 35 bar pressure. Before the CO_2 adsorption test, the sample was outgassed for 2 h at 250 °C, and a vacuum pump (Rocker 420, China) was used to evacuate the vessel filled with the sample. The adsorption experiments were carried out at pressures ranging from 1 to 25 bar at four different temperatures (15, 30, 45, and 75 °C). For determination of the dead volume of the whole setup, helium gas was used as non-adsorbing gas and expanded to the gas cell and then the adsorption cell. The total amount of CO_2 introduced into the system and remaining after reaching adsorption equilibrium was determined by measuring the volume of the gas cell, the CO_2 pressure before and after adsorption, and the temperature

of the system. Ultimately, the quantity of CO_2 adsorption by samples was evaluated by means of the Soave-Redlich-Kwong (SRK) equation of state using the MATLAB software (Heidari et al. 2014b).

Adsorption isotherms

The most commonly applied models to describe the experimental equilibrium data of adsorption isotherms are the Langmuir and the Freundlich models. The Langmuir equilibrium equation can be, then, described by the following nonlinear equation (Eq. 1) (Langmuir 1918):

$$q = q_m \left(\frac{bP}{1 + bP} \right) \tag{1}$$

where P is the equilibrium pressure, and q_m and b are the constants of the Langmuir isotherm. The Freundlich adsorption equation is an empirical model, frequently expressed as the following nonlinear equation (Eq. 2):

$$q = kP^n \tag{2}$$

where k and n are the adsorption capacity and the adsorption intensity, respectively (Jaroniec 1975).

Results and discussion

Properties of raw materials

The results of ultimate, proximate, and compound analyses of walnut shell powder according to the ASTM method are presented in Table 1. The high content of fixed carbon (17.76 wt%), volatile matter (67.18 wt%), and low value of ash content (3.48 wt%) proved that walnut shell biomass can be proposed an excellent candidate to utilize as a raw material for the synthesis of AC. However, the ultimate analysis illustrates the high content of C and O_2 in the structure of this precursor. The value of oxygen is directly associated with the content of the precursor's cellulose and hemicellulose and performs a key role in the CO_2 capacity of ACs (Valizadeh et al. 2016). In addition, the obtained results from

the compound analysis were also in accordance with the ultimate analysis and confirmed those (Heidari et al. 2014b; Nowrouzi et al. 2017b).

Thermogravimetric analysis

TGA analysis of walnut shells is depicted in Fig. 2. As expected and similar to the other lignocellulosic precursors, three main mass loss steps are observed with the enhancement of temperature: the first loss weight occurred at about 110 °C, indicating the evaporation of adsorbed moisture; the second and the extreme one was observed in the range from 210 to 380 °C with respect to the decomposition of hemicelluloses and organic matter; the third peak is recorded in 380–540 °C due to the lignin and cellulose decomposition (Nowrouzi et al. 2017a). Generally, it is confirmed that precursors with the high content of cellulose and hemicelluloses deserve to be utilized as a raw material to synthesis AC with the high CO_2 capacity and excellent final yield (Goel et al. 2016).
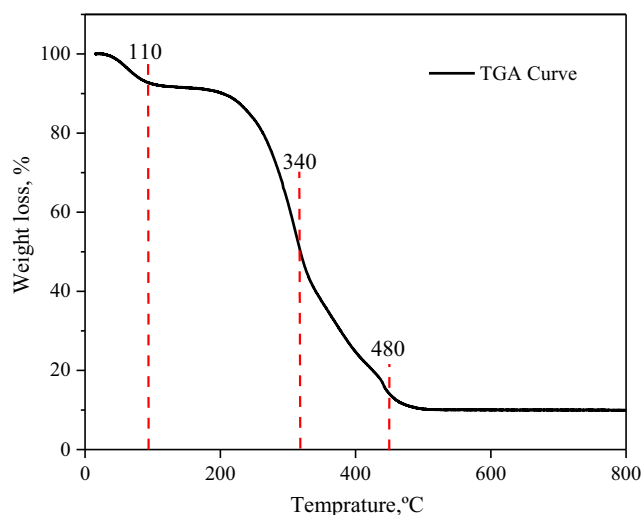
Porosity analysis test

The textural properties of ACs were determined by N_2 adsorption/desorption test. The obtained results are tabulated in Table 2. According to the IUPAC classification, the synthesized samples with KH as an activating agent followed type I, indicating the dominance of microporosity in their structure (Fig. 3). However, the samples manufactured with HP as an activating agent demonstrate a combination of types I and IV due to having a hysteresis loop at a pressure higher than 0.4 bars. This demonstrates the formation of mesoporosity, although microporosity is still dominated in the structure of ACs. Furthermore, the BJH and MP plot give a deep understanding concerning the distribution of porosity in the samples' structure (Fig. 3). These plots also proved the domination of microporosity over mesoporosity in the structure of synthesized ACs and were in good accordance with the aforesaid statements (Hesas et al. 2013).

It is noteworthy that the classification of porosity size is as follows: micropore (diameter < 2 nm), mesopore (2 < diameter < 50 nm), and macropore (diameter > 50 nm) (Nowrouzi et al. 2017b). According to Table 2, the majority of porosity in both samples with different activating agents were categorized

Table 1 Ultimate, proximate, and compound analysis of walnut shells powder (wt%, dry basis)

Proximate analysis	wt%	Ultimate analysis	wt%	Compound analysis	wt%
Moisture	11.57	Carbon	40.89	cellulose	28.88
Volatile matter	67.18	Hydrogen	0.7	Hemicellulose	26.21
Ash	3.48	Nitrogen	0.48	Lignin	38.12
Fixed carbon	17.76	Oxygen	57.83	Extractive material	6.09
		Sulfur	< 0.10		

Fig. 2 TGA analysis of walnut shells

Fig. 3 a Adsorption/desorption isotherms of N_2 at 77 K. b BJH pore size distribution and MP plot of synthesized sorbets
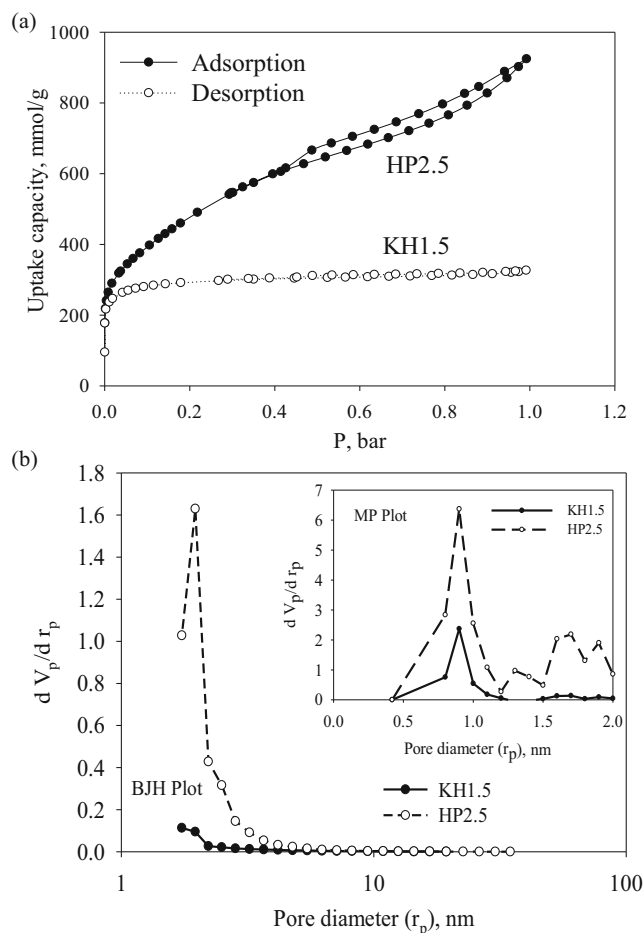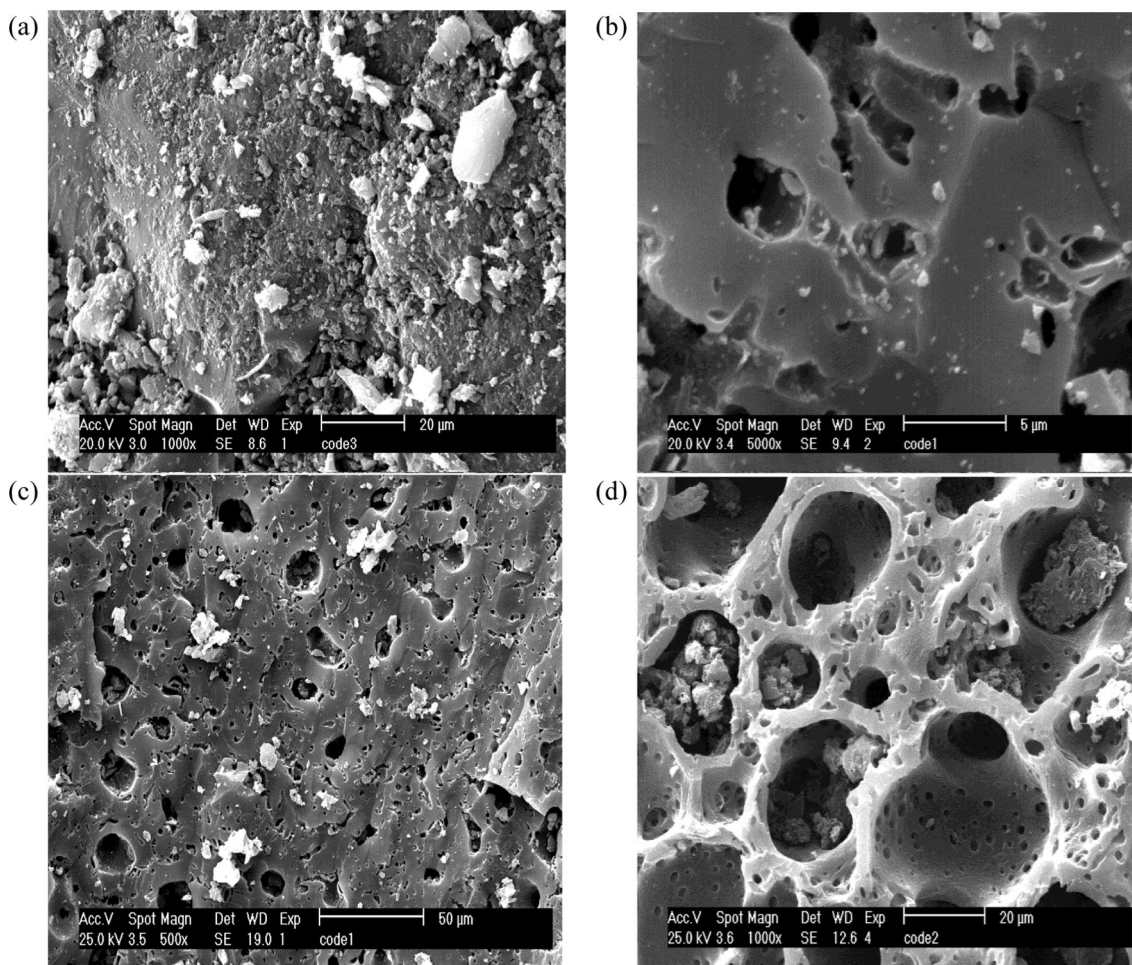
in micropore with the microporosity percentage of 74.65% and 90% for HP and KH, respectively. Considering the presented values for V_{mic} and V_{mes} in this table, HP intends to create and extend the mesoporosity, while the application of KH leads to the development of microporosity (Heidari et al. 2014b). Moreover, not only the porosity of samples but also their surface area are considered as a fundamental parameter in the CO_2 capture (Hesas et al. 2013). Thus, depending on the type and size of the adsorbates, in the large-scale application, a special type of activating agent should be utilized to achieve the maximum efficiency.

SEM analysis

The SEM images illustrate the occurred morphological changes in the structure of prepared ACs due to the application of HP and KH as activating agents in comparison with the raw precursor (Fig. 4). By heat treatment during the carbonization process, the available volatile organic matters in the structure of precursor are released and lead to the formation of numerous shrinkages and disintegrations. Obviously, the increase in temperature will be favorable up to optimum temperature and further one leads to the destruction of the AC structure and prevents the formation of a homogeneous cavity. According to the SEM images, the use of activating agents, e.g., KH and HP, has caused the development of porosity depending on their intrinsic properties and created the numerous cracks

and the small pits as expected. In addition, the clear white dots on the surface of AC are probably because of the presence of phosphate and potassium salt remains in the carbon structure (Heidari et al. 2014b; Nowrouzi et al. 2018). To attain more information in association with the available surface functional groups on the prepared ACs, FTIR analysis was carried out and the results are presented in the next section.

Surface functional groups

FTIR analysis was conducted to figure out the surface functional groups of synthesized ACs and their nature (Fig. 5). As can be observed, both spectra elucidated almost the same pattern with slight differences. For instance, two clear peaks

Table 2 Textural parameters of prepared ACs

Sample	Yield	Textural parameters					
		S_{BET} (m^2/g)	V_{mic} (m^3/g)	V_{mes} (m^3/g)	V_{tot} (m^3/g)	R_{mic} (nm)	$\%V_{mic}/V_{tot}$
HP2.5	46	1512.6	1.06	0.36	1.42	1.88	74.65
KH1.5	48	727.68	0.47	0.03	0.50	1.38	94

Fig. 4 SEM images of the AC samples derived from walnut shell biomass. **a** Precursor. **b** Carbonized carbon (600 °C). **c** KH1.5. **d** HP2.5

belong to the O–H stretching vibration due to the adsorption of water molecules onto ACs is assigned at 3445 cm^{-1} and 1632 cm^{-1} with different intensity (Nowrouzi et al. 2017a). Moreover, two smaller peaks at 2923 and 2848 cm^{-1} belong to C–H asymmetric stretching bond. The C=O stretching
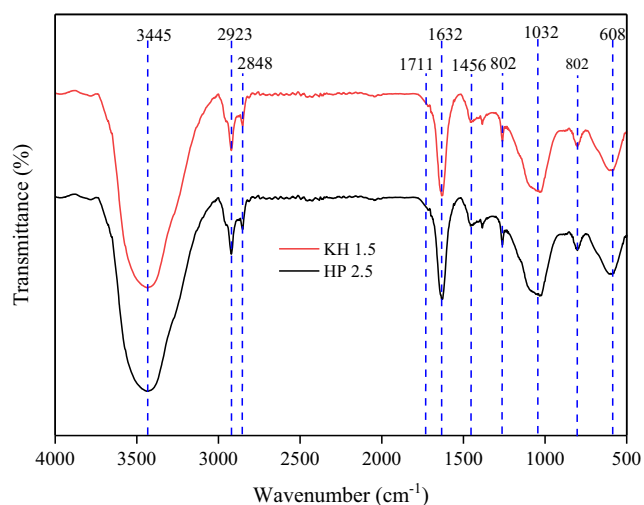

Fig. 5 FTIR spectra for the synthesized sorbets derived from walnut shell

vibration in lactones is obvious at 1711 cm^{-1}. The other identified peaks can be interpreted as follows: the –CH$_2$– deformation at 1456 cm^{-1} (Nowrouzi et al. 2018; Ozdemir et al. 2014), the asymmetric stretching vibrations of C–O–C in ethers at 1261 cm^{-1}, the stretching vibration of C–O at 1032 cm^{-1}, C–P bonding due to the existence of phosphine derivatives at 802 cm^{-1}, and the C–OH out-of-plane bending mode appeared at 608 cm^{-1} (Heidari et al. 2014b). Accordingly, the persistence of numerous surface functional groups, in particular, the basic ones, demonstrated that the synthesized ACs possess the high potential to adsorb acidic CO$_2$ molecules.

CO$_2$ adsorption optimization

The CO$_2$ adsorption capacity of the synthesized ACs is illustrated in Fig. 6. Briefly, the optimization process was carried out as follows: first of all, according to the results obtained from TGA analysis (Fig. 2), the precursor carbonizes at 600 °C. Afterward, by referring to the literature and corresponding to the activation temperature applied for the precursor with the same characteristics (Heidari et al. 2014b;
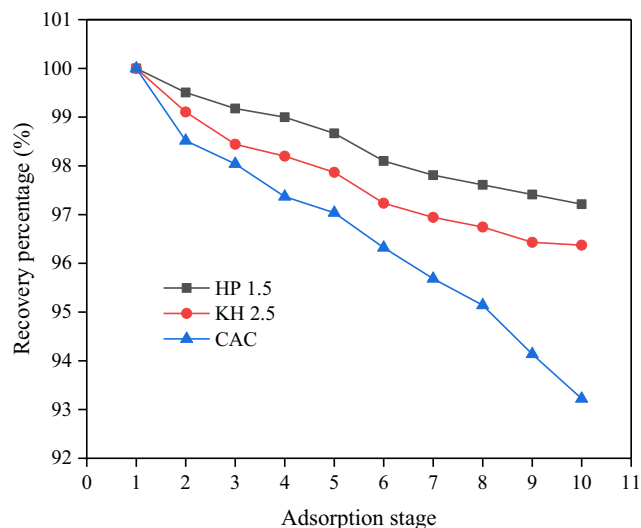
Fig. 6 CO_2 adsorption equilibrium isotherms at different ratios (**a**, **b**) and at various temperatures (**c**, **d**)
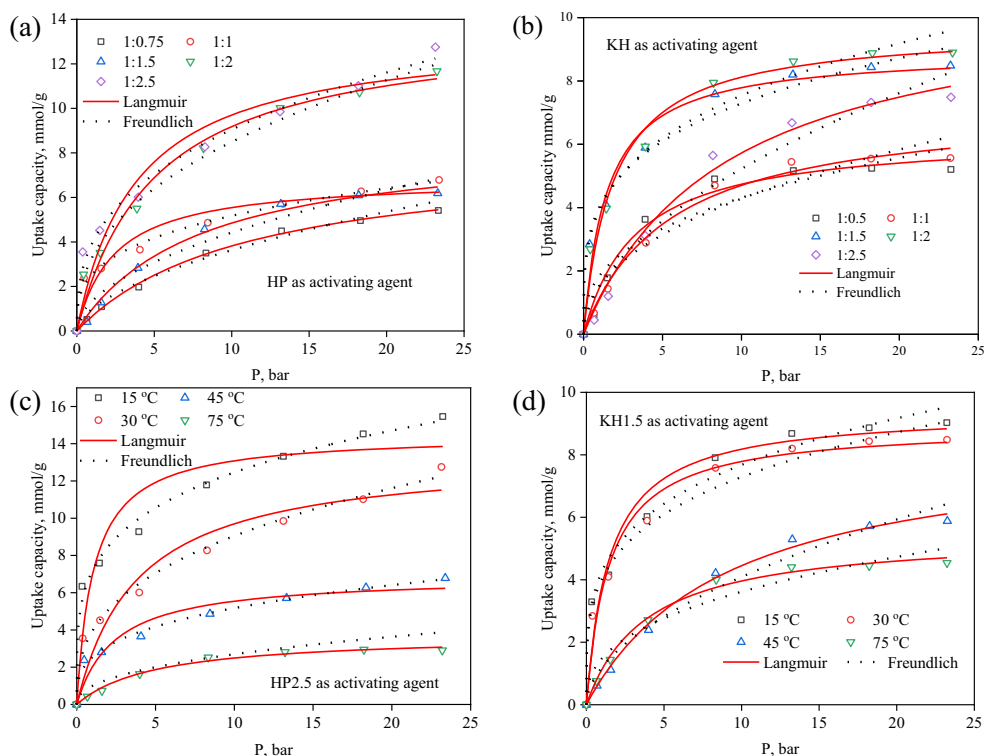
Nowrouzi et al. 2017b), the temperatures of 900 °C for activation with KH and 550 °C for HP were selected. Then, the optimization process according to the CO_2 adsorption capacity was performed at a mass ratio of the precursor to activating agents: 1:0.5 to 1:2.5 g/g for KH activation and 1:0.75 to 1:2.5 for HP one. According to the results, the highest CO_2 adsorption (at 1 bar and 30 °C) and S_{BET} were obtained for KH 1.5 and HP 2.5 (Fig. 6, Table 2).

In general, by increasing the activating agent ratios, CO_2 adsorption was rapidly raised at first in low pressures and then

Fig. 7 Successive adsorption/desorption cycles of CO_2 uptake at 1 bar and 30 °C

gradually decreased in higher pressures to reach the highest adsorption capacity (Heidari et al. 2014b; Yang et al. 2012). It can be described as follows: firstly, the plenty of vacant adsorption sites were available on the surface of adsorbents and easily filled by CO_2 molecules but by proceeding the reaction, the number of unsaturated sites was decreasing; hence, the rate of CO_2 adsorption reduced despite increasing pressure (Nowrouzi et al. 2018). According to Fig. 6, in the case of HP2.5, CO_2 adsorption was increased from 0.43 to 3.55 mmol/g at 1 bar and 30 °C by increasing the saturation ratio from 0.75 to 2.5 g/g. However, the same approach occurred concerning the KH1.5 up to 1:1.5 (precursor:activating agent) but decreased in higher saturation ratio. As mentioned, KH is responsible for the generation of micro- and sub-microporosity in the carbon structure, leading a considerable increment of S_{BET} (Ello et al. 2013). Obviously, the optimum CO_2 capture can be attained in a specific ratio of precursor:activating agent which causes the development of porosity. In verse, a further ratio not only has a negative effect on the CO_2 adsorption but also reduced it via the deconstruction of carbon's structure. Therefore, considering the significant role of microporosity and surface area in the CO_2 capture, every parameter that leads to the enhancement of these factors can play a positive influence on CO_2 adsorption. In addition, according to Fig. 6, CO_2 adsorption decreased by the enhancement of temperature, indicating the domination of physisorption during the CO_2 capture process. Hence, increase temperature provides sufficient energy to overcome the

Table 3 Equilibrium model constants for CO_2 adsorption by the synthesized sorbents

Activating agents	Saturation ratio	Temp. (°C)	Isotherm models					
			Langmuir			Freundlich		
			q_m	b	r^2	K_f	n	r^2
HP	0.75	30	7.99	0.09	0.99	0.97	1.77	0.99
	1	30	6.88	0.41	0.96	2.54	3.24	0.99
	1.5	30	8.65	0.12	0.99	1.34	3.24	0.98
	2	30	13.76	0.20	0.98	3.31	2.44	0.99
	2.5 (Op.)	15	14.49	0.92	0.97	4.18	7.18	0.99
		30	13.41	0.26	0.96	3.95	2.77	0.99
		45	6.88	0.41	0.96	2.54	3.24	0.99
		75	3.73	0.20	0.99	0.84	2.32	0.97
KH	0.5	30	6.30	0.30	0.99	1.84	2.70	0.95
	1	30	7.24	0.18	0.99	1.53	2.24	0.97
	2	30	9.65	0.52	0.99	4.40	4.09	0.95
	2.5	30	10.83	0.11	0.99	1.49	1.83	0.97
	1.5 (Op.)	15	9.40	0.66	0.97	4.74	4.60	0.95
		30	8.92	0.68	0.98	4.02	3.87	0.99
		45	8.37	0.11	0.99	1.17	1.87	0.98
		75	5.48	0.26	0.99	1.68	2.89	0.97
Carbonized	–	30	0.68	11.33	0.38	0.66	0.32	0.37
CAC	–	30	3.86	0.26	0.99	1.06	2.60	0.97

*Op.* optimized, *CAC* commercial activated carbon

available van der Waals forces among the adsorbed gas molecules and release those to the gas phase (Yang et al. 2012; Zhou et al. 2012). Moreover, the parallel increment of CO_2 adsorption and applied pressure proved that adsorption is an exothermic process. Generally, the sequence of CO_2 adsorption capacity at different temperatures for the synthesized ACs was as follows: 15 °C > 30 °C > 45 °C > 75 °C. The similar results were reported in the previous investigations (Heidari et al. 2014b; Nowrouzi et al. 2018).

Furthermore, in order to explore the potential of synthesized adsorbent regenerability, the adsorption/desorption test was conducted. The adsorbed CO_2 was regenerated under 250 °C for 2 h and at the same time, the pressure decreased to zero bar by a high-power vacuum pump after carrying out each cycle of adsorption. As displayed in Fig. 7, the CO_2 adsorption capacity of synthesized ACs decreased during 10 consecutive adsorption/desorption cycles. The decline rate of adsorption/desorption capacity during these cycles was as follows: 2.79, 3.63, and 6.76 for HP2.5, KH1.5, and CAC,

Table 4 Comparison of CO_2 adsorption capacity of the different ACs

AC source	Treatment method	Pressure (bar)	Temperature (°C)	Uptake capacity (mmol/g)	Refs.
African palm shells	Chemical/KOH (850 °C)	1	15	4.4	Ello et al. (2013)
Eucalyptus wood	Chemical/H_3PO_4/KOH (900 °C)	1	30	4.01	Heidari et al. (2014b)
Coconut shells	Chemical/KOH (800 °C)	2	15	2.55	Yang et al. (2011)
N-Doped AC	Chemical/H_3PO_4 (45 °C), ammonia modification (800 °C)	1	30	3.22	Heidari et al. (2014b)
Polysaccharides and sawdust	Chemical/KOH (600 °C)	1	15	4.80	Sevilla and Fuertes (2011)
Persian Ironwood	Chemical/KOH (800 °C)	1	30	3.77	Nowrouzi et al. (2017b)
Persian Ironwood	Chemical/H_3PO_4 (800 °C)	1	30	5.05	
HP2.5	Chemical/H_3PO_4 (550 °C)	1	30	3.55	This study
KH1.5	Chemical/KOH (900 °C)	1	30	2.84	This study
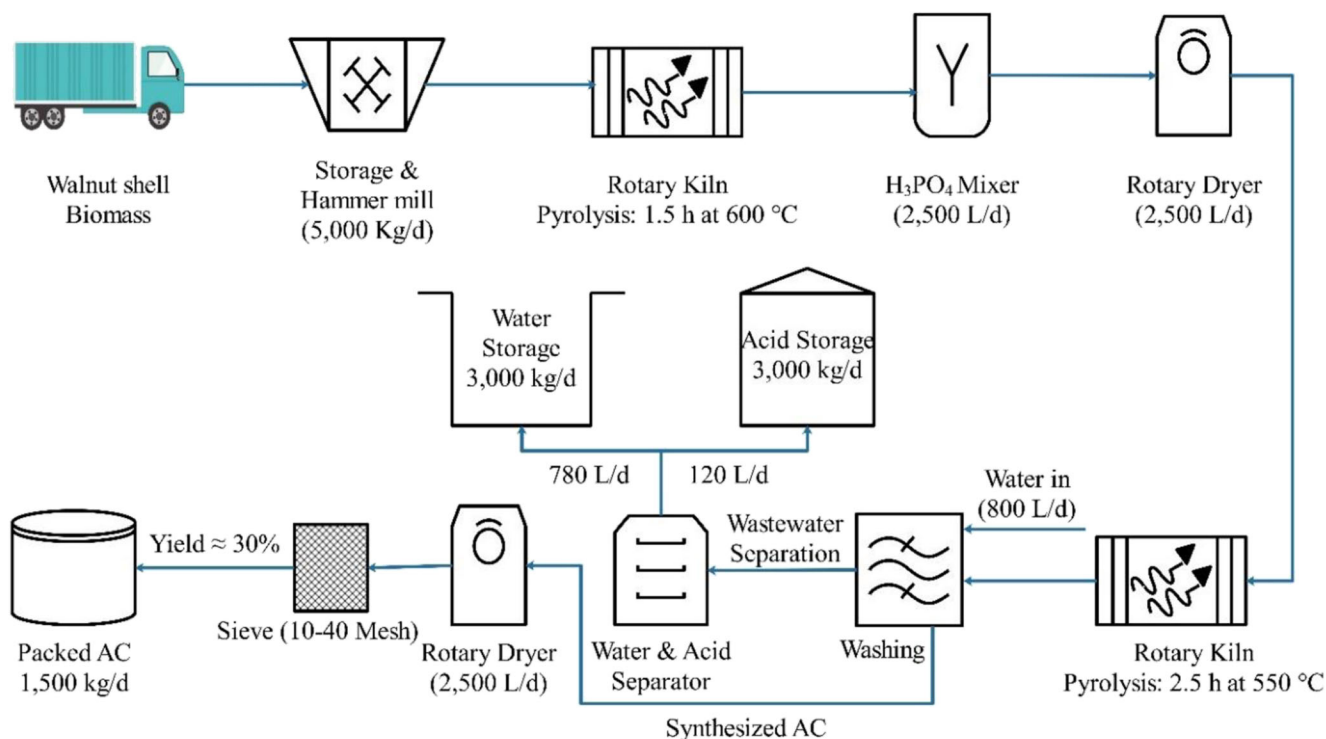
Fig. 8 Process flow diagram for the production of ACs from walnut shell

respectively. The slight decrease of adsorption capacity of prepared ACs can be due to the small changes in the structure of those in respect of the applied high-temperature vacuum to regenerate purpose (Heidari et al. 2014b). In general, dealing with the attained CO_2 adsorption capacity for CAC, the synthesized ACs by using both applied activating agents demonstrated not only the higher CO_2 adsorption capacity but also better regenerability potential. According to these findings, as-synthesized ACs demonstrated unique properties toward large-scale application.

CO_2 adsorption isotherms

To compare the obtained experimental data of adsorption with corresponding theoretical estimations at different temperatures and ratios, the most common equilibrium models, e.g., Langmuir and Freundlich model, were run out. According to Table 3 and the attained regression efficiencies, the samples synthesized by HP as an activating agent are more fitted with Langmuir model while those that are prepared with KH indicate the higher degrees of fitness with Freundlich model. A better fitness with Langmuir model confirms that CO_2 adsorption takes place as a monolayer onto the homogeneous surface, while the Freundlich model indicates the multilayer adsorption onto the heterogeneous surface (Valizadeh et al. 2016). Moreover, the *n* values that deal with Freundlich equation are greater than 1 in all cases, elucidating the tendency of adsorbent to capture adsorbate molecules. However, an

Table 5 Estimated capital cost for synthesis ACs from walnut shell

Equipment	Cost ($)
Transportation	3264
Storage and hammer mill	8424
Rotary dryer	32,128 each
Two-rotary kilns	85,247 each
Rotary mixer	55,830
Washing unit	46,325
Separator unit	54,561
Glass-lined, acid soak, and wash tanks	14,657
Acid and water storage tanks	12,948
Sieve	2282
Total equipment cost	1,012,211
Equipment installation	9146
Instrumentation	16,645
Piping and material transport (augers)	75,263
Electrical installation	19,823
Buildings	302,475
Yard improvements	92,634
Service facilities	216,255
Land	74,447
Engineering and supervision	157,327
Construction expense	422,296
Contractor's fee	19,718
Contingency	52,325
Total capital costs	2,903,606

available inverse trend of decreasing values of n with the increase of temperature demonstrated that the CO_2 adsorption performs with higher efficiency and in lower temperatures while higher temperatures provide the sufficient energy to overcome van der Waals force between adsorbent-adsorbate and return the adsorbent molecules to the gas phase. In addition, by rising temperature, the constant values of K_f were decreased, indicating the adsorption process was exothermic in nature (Yang et al. 2012). It is noteworthy that the maximum CO_2 adsorption capacity of synthesized samples (q_m) was calculated by Langmuir isotherm, and it decreased by enhancing temperature from 15 to 75 °C as follows: HP2.5 > KH1.5 > CAC.

Comparison of CO_2 adsorption

Nowadays, ACs are known as one of the most used widespread adsorbents in the post-combustion CO_2 capture. Therefore, extensive efforts are underway to identify the precursors with the highest efficiency of final yield and the most CO_2 adsorption capacity. The results of some of the previous investigations are tabulated in Table 4. Accordingly, it can be concluded that the ACs synthesized by the application of walnut shell possess an acceptable potential to utilize as an appropriate precursor for preparing AC to capture of CO_2.

Table 6 Annual operating costs for synthesis AC from walnut shell

Item	Annual cost ($)
Raw materials	
Walnut shell	178,321
Phosphoric acid	250,000
Utilities	
Lab	81,252
Water	146,365
Natural gas	4878
Electricity	16,682
Labor	
Operating labor	22,965
Maintenance labor	18,293
Supervision	29,872
Fringe benefits	6133
Supplies	
Operating supplies	98,324
Maintenance supplies	54,532
General works	
General and administrative	7685
Property insurance and tax	46,525
Depreciation	3224
Total cost	965,051

Table 7 Summary of costs for synthesis AC from walnut shell

Purchased equipment cost	$1,002,123
Total capital cost	$2,903,606
Total fixed capital investment	$1,124,356
Total annual operating cost	$965,051
Estimated annual production	435,000 kg
Estimated cost of AC	$1.83/kg

Cost analysis

Cost estimation of produced AC from walnut shells was conducted due to its low-cost and ease of accessing such a precursor to be potential adsorbent for CO_2 capture. This evaluation provides a benchmark to compare the ultimate cost of manufacturing AC derived from walnut shells rather than the other types of available CACs in the market. To attain this purpose, laboratory investigations accompanied by field surveys were performed to design a facile process with respect to the economic parameters effective onto the AC production. Moreover, the best performance coincident with the minimal cost is significantly depended on, in specific, the optimum size of the designed apparatus and the amount of applied precursor associated with the final yield (Nowrouzi et al. 2017b). Therefore, all assumed impressive parameters were tried to assess and apply to assure the final cost as elucidated in Fig. 8 and summarized in Tables 5, 6, and 7. By underestimating the final yield (i.e., 30%) to ensure the access, 300 days/year of production, and 2 labor force per shift (two shifts) for 24 h/day at $11/h, the estimated cost of AC production would be $1.83/kg. According to the best of our knowledge, the obtained price of ultimate production was significantly lower than the most of available ACs which are utilized to capture CO_2 in the same studies (Ng et al. 2003; Toles et al. 2000). Not only from the economical accepts, but also from the physical properties, as-synthesized AC in the current study demonstrated considerable advantages compared with the most available AC in the market (Heidari et al. 2014b; Nowrouzi et al. 2017b, 2018). As referenced in the last sections, these characteristics noticeably influenced the capacity of CO_2. Therefore, from an eco-environmental point of view and regarding the acceptable CO_2 capacity of synthesized ACs, walnut shells could be as a promising precursor for scale-up production of AC.

Conclusions

In the current study, a cost-effective AC derived from walnut shells with a high regenerability and an acceptable adsorption capacity for CO_2 capture is fabricated. The structural characteristics of ACs were determined by the different analyses,

indicating the excellent physio-chemical properties of prepared ACs. Furthermore, the optimization process was carried out in a wide range of pressures (1–25 bars), temperatures (15–75 °C), and activation ratios (0.5–2.5% *w/w*) of KH and HP. According to the obtained CO_2 adsorption capacity at the ambient pressure and 30 °C, the optimum ratios were 1:2.5 and 1:1.5 (precursor:activating agent), and the optimum temperatures were 550 and 900 °C for activating with HP and KH, respectively. Moreover, among all the synthesized ACs, HP2.5 elucidated the highest CO_2 capture with 3.55 mmol/g of CO_2 at 1 bar and 30 °C which was remarkably higher than that for CAC (1.67 mmol/g). However, the reversibility potential of HP2.5 decreased just about 2.79 after 10 consecutive adsorption/desorption tests at the aforementioned condition. In addition, physisorption was the dominating phenomenon to CO_2 capture and adsorption process was found to be spontaneous and exothermic in nature. The calculated price per kilogram of as-synthesized AC was about $1.83, indicating a highly competitive potential of synthesized AC in comparison with most of the available CAC in the market. Summing up, the present investigation demonstrated that walnut shell biomass could be efficiently utilized as an effective, low-cost, and eco-friendly source for CO_2 adsorption.

References

Ello AS, de Souza LK, Trokourey A, Jaroniec M (2013) Development of microporous carbons for CO_2 capture by KOH activation of African palm shells. J CO2 Util 2:35–38

Goel C, Kaur H, Bhunia H, Bajpai PK (2016) Carbon dioxide adsorption on nitrogen enriched carbon adsorbents: experimental, kinetics, isothermal and thermodynamic studies. J CO2 Util 16:50–63

Heidari A, Younesi H, Rashidi A, Ghoreyshi A (2014a) Adsorptive removal of CO_2 on highly microporous activated carbons prepared from *Eucalyptus camaldulensis* wood: effect of chemical activation. J Taiwan Inst Chem Eng 45:579–588

Heidari A, Younesi H, Rashidi A, Ghoreyshi AA (2014b) Evaluation of CO_2 adsorption with eucalyptus wood based activated carbon modified by ammonia solution through heat treatment. Chem Eng J 254:503–513

Hesas RH, Arami-Niya A, Daud WMAW, Sahu J (2013) Preparation and characterization of activated carbon from apple waste by microwave-assisted phosphoric acid activation: application in methylene blue adsorption. BioResources 8:2950–2966

Jaroniec M (1975) Adsorption on heterogeneous surfaces: the exponential equation for the overall adsorption isotherm. Surf Sci 50:553–564

Langmuir I (1918) The adsorption of gases on plane surface of glass, mica and platinum. J Am Chem Soc 40:1361–1403

Ng C, Marshall WE, Rao RM, Bansode RR, Losso JN (2003) Activated carbon from pecan shell: process description and economic analysis. Ind Crop Prod 17:209–217

Nowrouzi M, Behin J, Younesi H, Bahramifar N, Charpentier P, Rohani S (2017a) An enhanced counter-current approach towards activated carbon from waste tissue with zero liquid discharge. Chem Eng J 326:934–944

Nowrouzi M, Younesi H, Bahramifar N (2017b) High efficient carbon dioxide capture onto as-synthesized activated carbon by chemical activation of Persian Ironwood biomass and the economic pre-feasibility study for scale-up. J Clean Prod 168:499–509

Nowrouzi M, Younesi H, Bahramifar N (2018) Superior CO_2 capture performance on biomass-derived carbon/metal oxides nanocomposites from Persian ironwood by H_3PO_4 activation. Fuel 223:99–114

Ozdemir I, Şahin M, Orhan R, Erdem M (2014) Preparation and characterization of activated carbon from grape stalk by zinc chloride activation. Fuel Process Technol 125:200–206

Pal J, Deb MK (2014) Efficient adsorption of Congo red dye from aqueous solution using green synthesized coinage nanoparticles coated activated carbon beads. Appl Nanosci 4:967–978

Sevilla M, Fuertes AB (2011) Sustainable porous carbons with a superior performance for CO_2 capture. Energy Environ Sci 4:1765–1771

Toles CA, Marshall WE, Johns MM, Wartelle LH, McAloon A (2000) Acid-activated carbons from almond shells: physical, chemical and adsorptive properties and estimated cost of production. Bioresour Technol 71:87–92

Valizadeh S, Younesi H, Bahramifar N (2016) Highly mesoporous K_2CO_3 and KOH/activated carbon for SDBS removal from water samples: batch and fixed-bed column adsorption process. Environmental Nanotechnology, Monitoring & Management 6:1–13

Yang J, Qiu K (2010) Preparation of activated carbons from walnut shells via vacuum chemical activation and their application for methylene blue removal. Chem Eng J 165:209–217

Yang H, Gong M, Chen Y (2011) Preparation of activated carbons and their adsorption properties for greenhouse gases: CH_4 and CO_2. J Nat Gas Chem 20:460–464

Yang R, Liu G, Li M, Zhang J, Hao X (2012) Preparation and N_2, CO_2 and H_2 adsorption of super activated carbon derived from biomass source hemp (*Cannabis sativa* L.) stem. Microporous Mesoporous Mater 158:108–116

Zhou X, Yi H, Tang X, Deng H, Liu H (2012) Thermodynamics for the adsorption of SO_2, NO and CO_2 from flue gas on activated carbon fiber. Chem Eng J 200:399–404